

Enhancement of poly(ethylene glycol) mucoadsorption by biomimetic end group functionalization

Nathaniel D. Catron

Materials Science and Engineering Department, Northwestern University, 2220 Campus Drive, Evanston, Illinois 60208

Haeshin Lee

Biomedical Engineering Department, Northwestern University, 2145 Sheridan Road, Evanston, Illinois 60208

Phillip B. Messersmith^{a)}

Biomedical Engineering Department, Northwestern University, 2145 Sheridan Road, Evanston, Illinois 60208 and Materials Science and Engineering Department, Northwestern University, 2220 Campus Drive, Evanston, Illinois 60208

(Received 25 October 2006; accepted 11 November 2006; published 17 January 2007)

Poly(ethylene glycol) (PEG) is widely used in the pharmaceutical, biotechnology, and medical device industries. Although PEG is a biocompatible polymer that has enjoyed widespread use in drug delivery technology, it is not considered adhesive toward mucosal tissue. Here the authors describe a simple approach to enhancing mucoadsorption of PEG polymers through end group functionalization with the amino acid 3,4-dihydroxyphenyl-L-alanine (DOPA). Using a variety of surface analytical techniques, the authors show that a four-armed poly(ethylene glycol) polymer functionalized with a single DOPA residue at the terminus of each arm (PEG-(DOPA)₄) adsorbed strongly to surface immobilized mucin. Successful mucoadsorption of PEG-(DOPA)₄ across several pH values ranging from 4.5 to 8.5 was demonstrated, and control experiments with unfunctionalized four-arm PEG demonstrated that mucoadsorption of PEG-(DOPA)₄ is due largely to the presence of DOPA end groups. This conclusion was confirmed with single molecule atomic force microscopy experiments that revealed a surprisingly strong interaction force of 371 ± 93 pN between DOPA and adsorbed mucin. Direct comparisons with known mucoadhesive polymers revealed that PEG-(DOPA)₄ was equal to or more adsorptive to immobilized mucin than these existing mucoadhesive polymers. In addition to demonstrating significant enhancement of mucoadhesive properties of PEG by DOPA functionalization, this study also introduced a new simple approach for rapid screening of mucoadhesive polymers. © 2006 American Vacuum Society. [DOI: 10.1116/1.2422894]

I. INTRODUCTION

The surfaces of mucosal tissues are important biointerfaces across which many clinical drug delivery strategies operate. In recent years there has been growing interest in the delivery of therapeutics to the mucosal membranes of the gastrointestinal and reproductive tracts, as well as the surface of the eye.^{1,2} Mucoadhesive drug carriers offer the potential to improve the bioavailability of drugs through increased retention time at the site of delivery, prolong drug delivery, and reduce the required dosage or dosage frequency.² Mucoadhesive compounds have been developed for drug delivery to ocular,³ nasal,⁴ buccal,⁵ and vaginal⁶ tissues.

Although much emphasis has been placed on the discovery of polymers that are inherently mucoadhesive,⁷ little molecular understanding of polymer-mucin interactions exists and to date there remains only a small pool of known mucoadhesive polymers such as poly(acrylic acid) (PAA),⁸ chitosan,⁹ and the GantrezTM polymer family.¹⁰ Of these, many exhibit pH-dependent mucoadhesion properties.^{7,11} For example, PAA shows optimal mucoadhesion at pH of 4–5

and greatly reduced mucoadhesion at higher pH values⁸. Because of these and other limitations there exists a great need for new mucoadhesive polymers that possess superior encapsulation ability, enhanced delivery performance, or improved biocompatibility. Introduction of chemical functional groups capable of strong interactions with mucin has been shown to be a viable approach to enhancing mucoadhesion of polymers. For example, it has been shown that the adhesive properties of PAA (Ref. 12) and chitosan¹³ have been improved through functionalization with thiol groups. Poly(ethylene glycol) (PEG) has been reported to be nonmucoadhesive,^{7,14} although in the form of hydrogels¹ and when copolymerized with acrylate polymers,¹⁵ PEG has been shown to enhance mucoadhesion.

Several strategies for testing mucoadhesion of synthetic polymers have been developed;^{16,17} however, most are based on macroscopic or microscopic methods and yield few details on the molecular level.¹⁸ An atomic force microscopy (AFM)-based approach was used by Cleary *et al.* to probe the interaction force between a mucoadhesive polymer coated sphere and mucin⁸.

Mussel adhesive proteins (MAPs) are interesting models for adhesive polymers, and in fact purified MAPs have been

^{a)}Author to whom correspondence should be addressed; electronic mail: philm@northwestern.edu

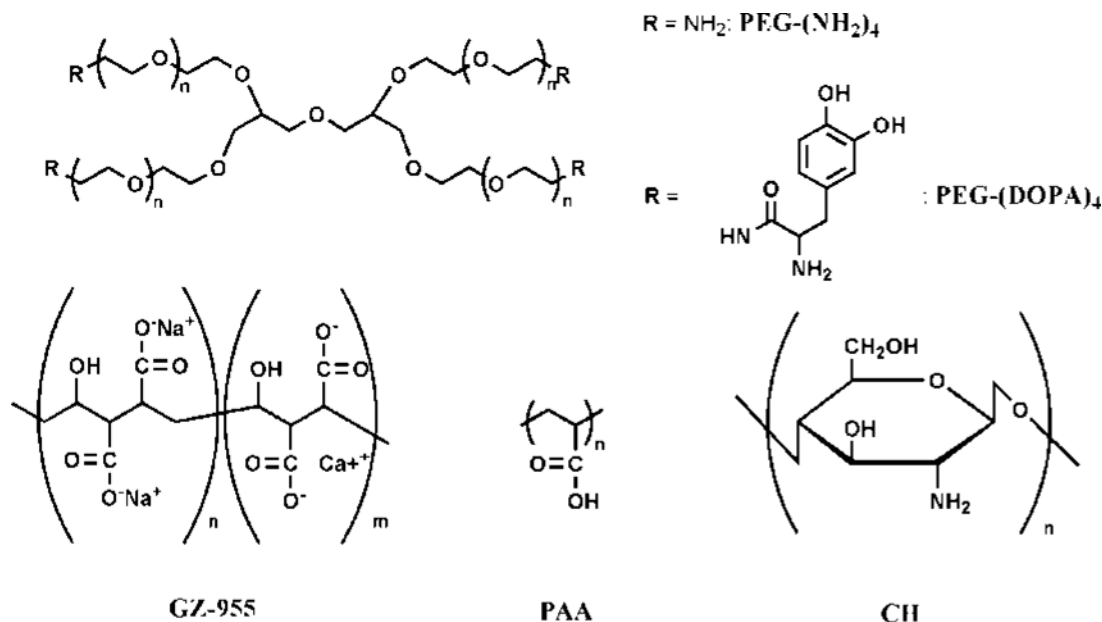


FIG. 1. Chemical structures of PEG-(NH₂)₄, PEG-(DOPA)₄, GZ-955, PAA, and CH.

previously reported to be highly mucoadhesive^{19,20}. Although strong interactions between mucin and whole proteins extracted and purified from mussel adhesive plaques were found, the complexity inherent to whole proteins prevented the authors from attributing the observed mucoadhesive behavior to specific residues or functional groups present in the MAPs. Inspired by these earlier reports, we are designing MAP mimetic polymers for interaction with mucin. A general strategy that we have previously reported^{21,22} involves attachment of 3,4-dihydroxy-L-phenylalanine (DOPA), the amino acid believed to be most responsible for interfacial adhesion of MAPs,^{23–25} to polymer chain ends.

Here we report the mucoadhesion relevant properties of a PEG polymer chemically modified with DOPA. Mucin proteins were adsorbed onto metal oxide surfaces and used as model mucous membranes for adhesion experiments at a variety of pH conditions. Spectroscopic ellipsometry, x-ray photoelectron spectroscopy (XPS), and optical waveguide light mode spectroscopy (OWLS) were used to characterize deposition of mucin and PEG polymer, and AFM was used to measure the force of interaction between a single DOPA residue and mucin. Our results show that DOPA is highly mucoadhesive and its incorporation in a PEG polymer, in even small amounts, greatly enhances mucoadsorption of PEG.

II. EXPERIMENT

Materials. The chemical structures of the DOPA modified PEG polymer and the four existing mucoadhesive polymers used for comparison are shown in Fig. 1. 4-arm-poly(ethylene glycol)-amine [PEG-(NH₂)₄, $M^w=10\,000$] was purchased from SunBio, Inc. (Walnut Creek, CA). 4-arm-poly(ethylene glycol)-DOPA [PEG-(DOPA)₄, $M^w=11\,400$] was synthesized as described previously²¹ from PEG-(NH₂)₄ and stored at $-4\text{ }^\circ\text{C}$ in a vacuum dessicator. Gantrez MS-955

(GZ-955, $M^w=1\,000\,000$) was provided as a free sample from ISP Chemicals (Columbus, OH). Bovine submaxillary mucin (BSM), poly(acrylic acid) (PAA, $M^w=450\,000$), low molecular weight chitosan (CH), sodium citrate, sodium acetate, Tris buffer, and HEPES buffer were obtained from Sigma-Aldrich (St. Louis, MO) and were used as received. Water used for all experiments was purified with a Millipore water treatment apparatus [$\geq 18.2\text{ M}\Omega\text{ cm}$, total organic content $\leq 5\text{ ppb}$].

Surfaces and surface preparation. Silicon wafers (University Wafer, Boston, MA) were coated with 20 nm of TiO₂ by physical vapor deposition using electron beam evaporation (Edwards Auto306; $<10\text{--}5\text{ Torr}$) with a TiO₂ target. The coated wafers were then cut into $1\times 1\text{ cm}$ pieces for ellipsometry measurements. Optical waveguide substrates (Microvacuum Ltd., Budapest, Hungary) were similarly coated with 8 nm of TiO₂. The waveguides consisted of an AF45 glass substrate ($8\times 12\times 0.5\text{ mm}^3$) with a 200 nm thick Si_{0.25}Ti_{0.75}O₂ waveguiding surface layer before TiO₂ coating. Prior to use, all substrates were sonicated for 10 min in 2-propanol, dried in a stream of N₂, and then exposed to O₂ plasma (Harrick Scientific, Ossining, NY) for 3 min. Waveguides were regenerated for reuse by sonicating in 0.1N HCl and water for 10 min each, and then sonicated in 2-propanol and plasma cleaned immediately prior to use.

Surface modification. To create a mucin surface for polymer adsorption experiments, BSM was allowed to adsorb to a freshly cleaned TiO₂ surface overnight in a 37 °C incubator at a concentration of 1 mg/ml in HEPES buffer (10 mM, pH of 7.4). The surfaces were then rinsed gently with water and dried with a stream of N₂ gas and immediately used in an adhesion experiment. For adhesion experiments, mucin coated substrates were exposed to a solution of PEG-(NH₂)₄, PEG-(DOPA)₄, PAA, CH, or GZ-955 polymer at a concen-

tration of 10 mg/ml in buffer for 1 h at 37 °C, and then rinsed with the matching buffer. The buffers used were as follows: 10 mM acetate, pH of 4.5; 10 mM citrate, pH of 6.0; 10 mM HEPES, pH of 7.4; and 10 mM Tris, pH of 8.5.

Spectroscopic ellipsometry. Ellipsometry (ELM) measurements were performed on TiO₂ coated Si wafers, prepared as described above. Substrates were analyzed twice, once after incubation with HEPES buffer and once after mucin adsorption. The substrates were rinsed with water and dried with N₂ prior to scanning. ELM was performed on M-2000D spectroscopic ellipsometer (J. A. Woollam Co., Inc., Lincoln, NE) at 65°, 70°, and 75° using wavelengths from 193 to 1000 nm. The data were then fitted to a multilayer model using the instrument software. The properties of a general Cauchy polymer layer²⁶ were used to determine the thickness of the adsorbed mucin. The thickness reported is from a sample size of 20 substrates.

Optical waveguide light mode spectroscopy. OWLS is a surface analysis technique that allows highly accurate, real-time examination of adsorption processes at the liquid-surface interface.²⁷ Detection limits of this system are on the order of 1 ng/cm². TiO₂ coated waveguides were cleaned in 2-propanol and O₂ plasma as described above. Clean waveguides were placed in a solution of BSM and incubated overnight at 37 °C. Before experiments were performed, the waveguides were rinsed with water and dried gently with N₂ and placed in the flow cell of the measurement head of an OWLS110 (Microvacuum Ltd.), where temperature was maintained at 37 °C at all times. Mucin coated waveguides were stabilized for at least 1 h in the buffer corresponding to the pH to be tested. After equilibration a solution of PEG-(NH₂)₄, PEG-(DOPA)₄, CH, PAA, or GZ-955 was injected in a stop flow mode. After monitoring polymer adsorption the flow cell was purged with buffer to remove any unbound polymer. The system was allowed to stabilize after the final buffer rinse where a final value for adsorbed mass was obtained. Manufacturer supplied software then converted the raw data to adsorbed mass in units of ng/cm² using the formula of Feijter *et al.*²⁸ The refractive index increment, dn/dc , was determined for each polymer via a refractometer (Rudolph Research J157 refractometer, Hackettstown, NJ). OWLS experiments were performed at least twice for PEG-(NH₂)₄ and at least four times for each mucoadhesive polymer at each pH value.

X-ray photoelectron spectroscopy (XPS). XPS analyses were performed on an Omicron ESCALAB (Omicron, Taurusstein, Germany) with a monochromated Al K α (1486.8 eV) 300 W x-ray source, with a flood gun to counter charging effects. Unless otherwise noted, all data were collected using a takeoff angle (defined as the angle between surface normal and detector) of 45°, at bandpass energies of 50 and 14 eV for survey and high resolution scans, respectively. All data obtained were referenced to the hydrocarbon peak of C 1 s, located at 284.7 eV. High resolution C 1 s scans were taken at varying takeoff angles (5°–85°) and CASAXPS software was used to curve fit the components using a Shirley background subtraction and the sum of a 90%

Gaussian and 10% Lorentzian function. Angle-dependent measurements were used to build only a qualitative depth profile, given that the thickness of each polymer/protein layer was small compared to the mean free path of the electrons in those layers.

Atomic force microscopy (AFM). AFM cantilevers (silicon nitride, Veeco probe SN-40) were modified with DOPA via a PEG tether as described in our previous work.²⁹ Briefly, cantilevers were cleaned in a piranha solution (sulfuric acid: H₂O₂=8:2) for 30 min. After extensive rinsing with nanopure H₂O, the cantilevers were transferred into 20% (v/v) 3-aminopropyltrimethoxysilane in toluene for 30–60 min, resulting in an aminosilane functionalized tip. The aminated tips were then functionalized with a mixture of methoxy-PEG-*N*-hydroxy succinimide (mPEG-NHS, M_w =2000, Nektar Inc.) and Fmoc-PEG-*N*-hydroxy succinimide (Fmoc-PEG-NHS, M_w =3400, Nektar Inc.) at a ratio of Fmoc-PEG-NHS:mPEG-NHS=1:15. The Fmoc protecting groups were cleaved by treatment of the tips in 20% piperidine (v/v in *N*-Methyl-2-Pyrrolidone (NMP)) for 0.5 min, followed by coupling of *N*-Boc-DOPA to the liberated amine in Benzotriazole-1-yl-oxy-tris-(dimethylamino)-phosphonium hexafluorophosphate/1-Hydroxybenzotriazole/DOPA (molar ratio of 1:1:1, 8 mM in NMP) solution with 10 μ l DIPEA. Separately, we prepared mPEG (2 kDa) immobilized cantilevers for control experiments. The PEG functionalization was performed at a total PEG concentration of 5 mM in 50 mM sodium phosphate buffer, pH of 7.8 at room temperature, and subsequently repeated in chloroform at room temperature for 3 h using only mPEG-NHS. The equipartition theorem was used to determine the spring constant of each silicon nitride cantilever by measuring its resonance frequency (10–50 kHz).³⁰ Force-distance curves were obtained at a pulling rate of 1 μ m/s with no time delay between approach and retract portions of the experiment. The maximum applied force between cantilever and surface during approach was 15 nN. All measurements were performed in buffer at four different pH conditions: 10 mM acetate, pH of 4.5; 10 mM citrate, pH of 6.0; 10 mM HEPES, pH of 7.4; and 10 mM Tris, pH of 8.5.

III. RESULTS AND DISCUSSION

Mucin layer deposition onto TiO₂. We first developed a simple model that would allow rapid screening of candidate mucoadhesive polymers. As a first approximation of a mucous membrane, we created an adsorbed layer of BSM by immersing freshly cleaned TiO₂ coated substrates in a solution of BSM overnight in a 37 °C incubator. TiO₂ was used as the supporting substrate for the mucin thin film in part because of its known chemical signature in XPS and compatibility with the OWLS technique and also because the strength of its interaction with DOPA is quantitatively known, which allowed us to eliminate the possibility that observed PEG-(DOPA)₄ adsorption onto the mucin layer could be explained by interaction between DOPA and TiO₂ surface (see discussion on AFM below). After rinsing and drying the mucin coated TiO₂, we determined using ellip-

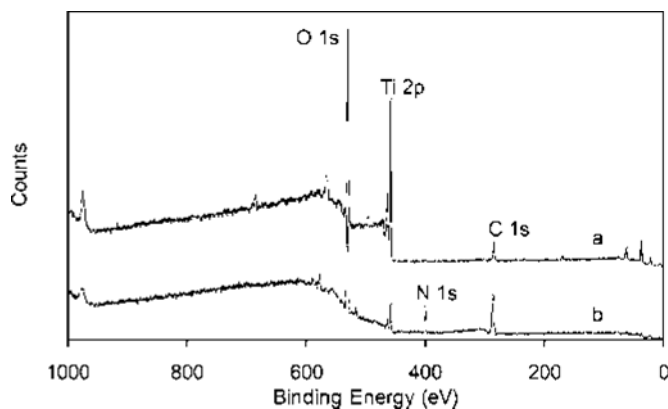


FIG. 2. XPS survey scans of (a) TiO_2 coated Si wafer and (b) TiO_2 coated Si wafer with adsorbed mucin.

sometry that 4.3 ± 0.9 nm of mucin had adsorbed. This value agrees well with adsorbed mucin thicknesses published by Shi and Caldwell (3.5–4 nm) in their study of mucin as an antifouling coating.³¹

XPS was used to further confirm mucin adsorption onto the TiO_2 surface. XPS spectra of TiO_2 before and after adsorption of mucin are shown in Fig. 2. The unmodified TiO_2 had a spectrum typical of Ti substrates, with titanium, oxygen, and some hydrocarbon contaminant peaks present.³² The XPS spectra of mucin coated TiO_2 exhibited a nitrogen 1s peak (400.5 eV) due to the presence of mucin, and also exhibited attenuated Ti 2p peaks (459 and 465 eV) consistent with an adsorbed mucin layer that is thin relative to the mean free path of the electrons in mucin. Within the high resolution spectrum of the C 1s region [Fig. 3(a)], amide carbon (288.2 eV), ether carbon (286.5 eV), and hydrocarbon (284.7 eV) peaks were observed. These results are consistent with the known repeat unit structure of mucin,¹ which consists of a protein backbone with branched polysaccharide side chains that include ether carbon and hydrocarbon moieties.

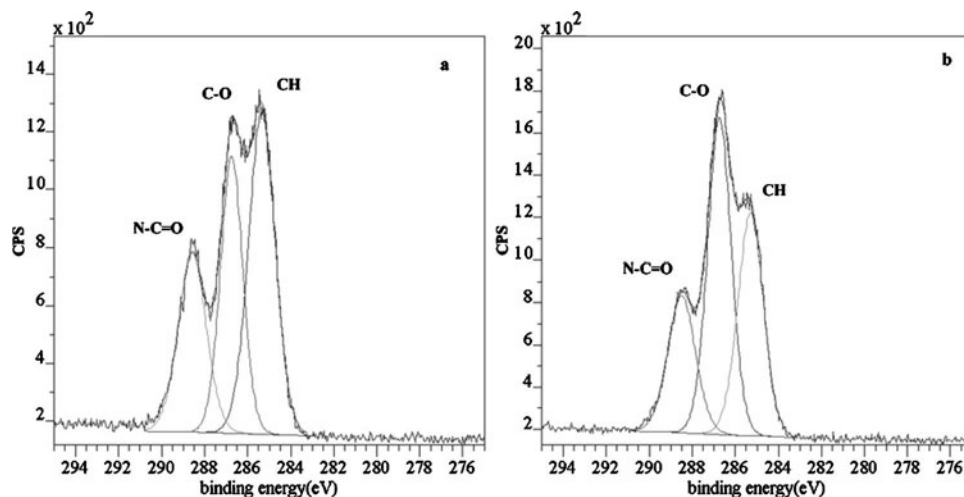


FIG. 3. High resolution C 1s scans of (a) TiO_2 coated Si wafer with adsorbed mucin and (b) TiO_2 coated Si wafer with adsorbed mucin and adsorbed PEG-(DOPA)₄.

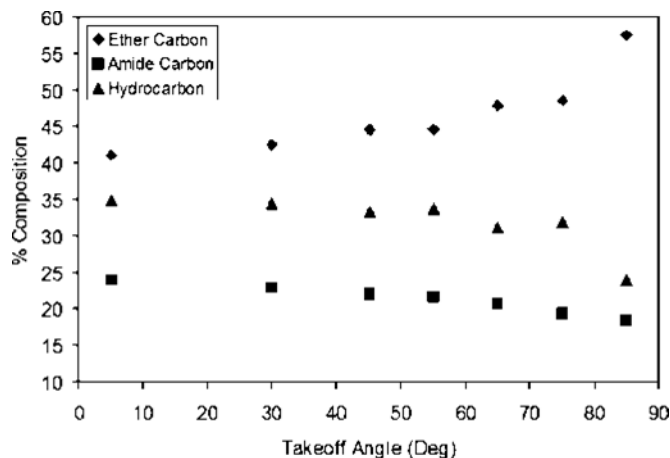


FIG. 4. Percent composition of XPS C 1s peak components vs takeoff angle for the case of PEG-(DOPA)₄ adsorbed to a mucin layer on a TiO_2 coated Si wafer.

Mucoadsorption of PEG-(DOPA)₄. Exposure of the mucin coated TiO_2 surfaces to a solution of PEG-(DOPA)₄ resulted in polymer adsorption as confirmed by XPS. Upon exposure to PEG-(DOPA)₄ for 1 h, the XPS spectra were significantly changed [Fig. 3(b)]. The changes were most pronounced in the C 1s region, with the ether carbon peak increasing greatly with respect to the amide and hydrocarbon peaks due to presence of the PEG polymer. Qualitative information on the layered structure of the mucin and PEG-(DOPA)₄ coating was revealed through angle-dependent XPS measurements. A plot of relative C 1s component (ether, amide, hydrocarbon) intensity versus takeoff angle is shown in Fig. 4. Takeoff angle is defined as the angle between surface normal and detector, thus higher angle refers to a shallower sampling depth. It can be clearly seen that as the sampling depth gets shallower, the ether carbon intensity increases at the expense of the amide and hydrocarbon components, qualitatively indicating that the PEG-(DOPA)₄

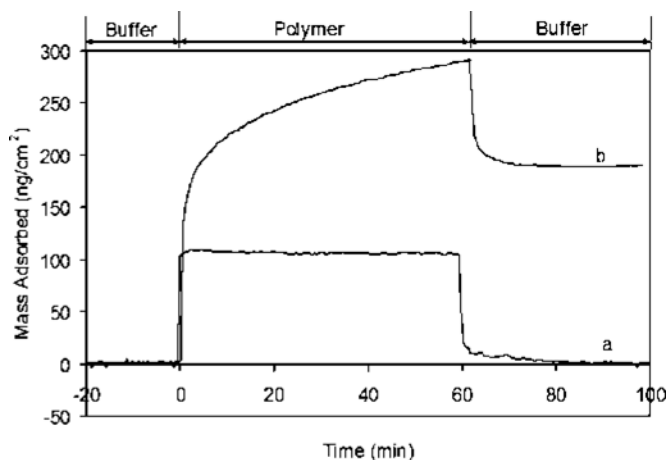


FIG. 5. OWLS traces showing mass adsorbed vs time for interaction of a solution containing (a) PEG-(NH₂)₄ and (b) PEG-(DOPA)₄ with a mucin coated TiO₂ waveguide. The polymer solution concentration in both cases was 10 mg/mL in 10 mM HEPES, pH of 7.4.

polymer is adsorbed on top of the mucin layer.

OWLS was used to further probe the mucoadhesive properties of PEG-(DOPA)₄ by adsorbing mucin onto waveguides. Pristine TiO₂ coated OWLS waveguides were modified overnight with mucin as described above and then used to determine the mass of PEG-(DOPA)₄ adsorbed. A representative set of OWLS experiments is shown in Fig. 5. The data show a rapid initial rise in signal as a result of the change in covering medium index of refraction due to the exchange of buffer with PEG-(DOPA)₄ containing buffer.²⁷ Similarly, at time $t=60$ min there is a rapid signal decrease when the medium in the flow cell is returned to the original buffer. The final adsorbed mass of polymer is taken as the plateau value at the conclusion of a buffer rinse. In the absence of DOPA end groups, PEG-(NH₂)₄ shows little or no interaction with the mucin layer as evidenced by the flat response in the curve and return to base line after exchange with buffer. This result is consistent with previous literature reports demonstrating that PEG is not highly mucoadhesive.^{7,14} In the representative curves shown in Fig. 5, the PEG-(NH₂)₄ control showed virtually no detectable adsorption, whereas approximately 190 ng/cm² of PEG-(DOPA)₄ adsorbed during the same time period.

Figure 6 compares the amounts of PEG-(DOPA)₄, PAA, CH, and GZ-955 that adsorbed onto BSM coated TiO₂ at pH of 4.5 in 10 mM acetate buffer. Existing mucoadhesive polymers PAA, CH, and GZ-955 were all found to adsorb to the immobilized mucin surface with average values of 112, 60, and 52 ng/cm², respectively. This result, along with the lack of adsorption of PEG-(NH₂)₄ under identical conditions (15 ng/cm², not shown), provided some measure of validation that the TiO₂ immobilized mucin serves as a reasonable model system for screening mucoadhesive polymers. Importantly, it was found that under identical conditions, PEG-(DOPA)₄ adsorbs to immobilized BSM at a greater level than both GZ-955 and CH ($p < 0.004$ and $p < 0.01$, respectively) and equal to PAA.

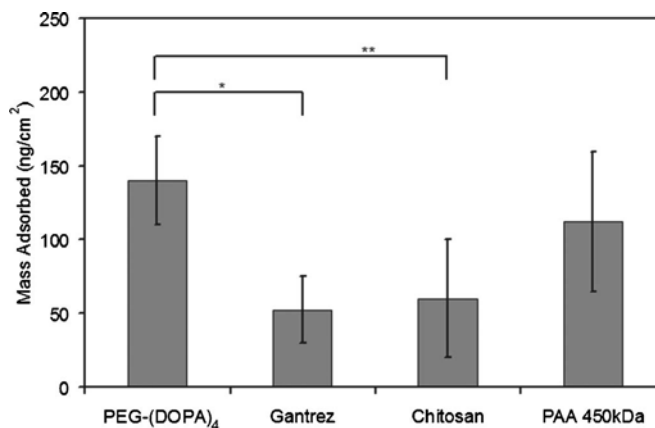


FIG. 6. OWLS results for mass of mucoadhesive polymer adsorbed to mucin coated TiO₂ at pH of 4.5 [^{*} $p < 0.004$, (^{**}) $p < 0.01$].

pH dependence of PEG-(DOPA)₄ mucoadsorption. It is well established that existing mucoadhesive polymers often show pH-dependent behavior, with optimal mucoadhesion typically occurring only over a limited pH range.^{1,7} In order to determine if this was also the case for PEG-(DOPA)₄, the pH dependence of PEG-(DOPA)₄ mucoadsorption was explored in greater detail by performing OWLS experiments at pH of 4.5, 6.0, 7.4, and 8.5. Our results, as summarized in Fig. 7, show that mucoadsorption of PEG-(DOPA)₄ was high throughout the entire pH range studied, with a maximum adsorption of greater than 200 ng/cm² at pH of 6.0. For comparison, the OWLS adsorptions of GZ-955 (Ref. 10) and PEG-(NH₂)₄ were performed at the same pH values and both polymers were found to be significantly less mucoadsorptive than PEG-(DOPA)₄ at all pH values.

The OWLS approach used here bears some resemblance to the surface plasmon resonance (SPR) approach employed by Takeuchi *et al.* to investigate interactions between immobilized polymers and mucin particles in suspension.¹⁷ Unlike the SPR method, however, OWLS is capable of direct mass detection and is somewhat more flexible with substrate composition as it does not require a gold sensor surface.²⁷ The OWLS method may therefore prove to be a useful alternative to SPR for studying mucoadhesion.

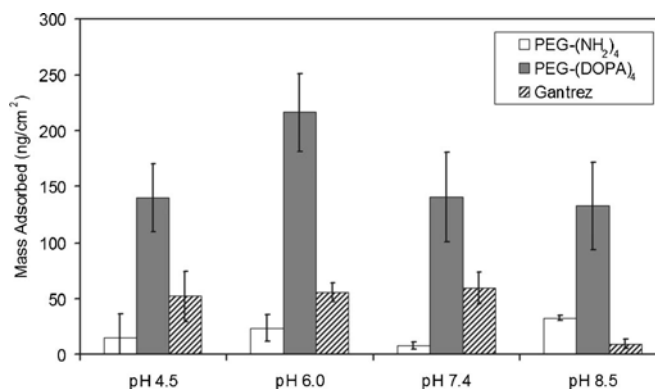


FIG. 7. OWLS results for mass of mucoadhesive polymer adsorbed to mucin coated TiO₂ at a variety of pH values.

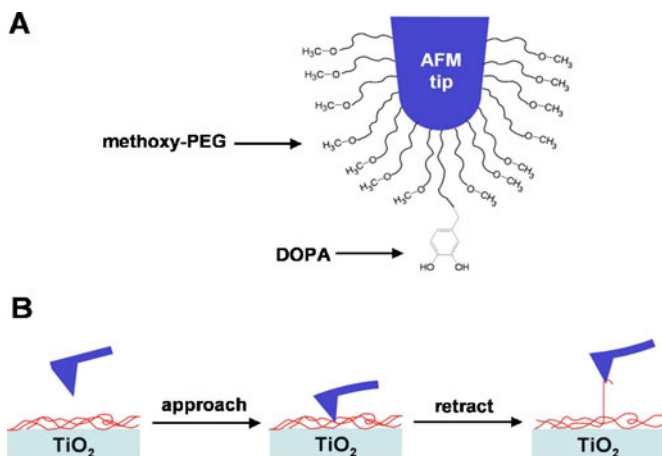


FIG. 8. Schematic illustration of DOPA-mucin AFM experiment. (A) Representation of a covalently modified AFM tip showing a DOPA functionalized PEG chain amidst an excess of methoxy terminated PEG. (B) F - D curves were obtained by approach of modified AFM tips to a mucin coated TiO_2 substrate followed by retraction away from the surface.

AFM force measurement of DOPA-mucin interaction. The strength of interaction between DOPA and adsorbed mucin was probed by measuring the force necessary to dissociate a DOPA modified AFM tip from a mucin coated TiO_2 substrate. The tips were prepared according to our previously published protocol which yields a single DOPA residue covalently coupled to an AFM cantilever via a 3.4 kDa PEG tether.²⁹ As schematically illustrated in Fig. 8, the method results in a large excess of methoxy terminated PEG on the tip, such that the probability of observing more than one DOPA residue per tip is low.²⁹ The tethered PEG chains with terminal DOPA residues bear resemblance to each arm of the $\text{PEG}-(\text{DOPA})_4$ molecule, and therefore this AFM approach comes close to approximating $\text{PEG}-(\text{DOPA})_4$ as it interacts with mucin.

In our previous work we showed that a single DOPA residue exhibited a reversible binding force of ~ 800 pN on TiO_2 substrates.²⁹ To employ this approach for determining DOPA-mucin interaction force we began by first confirming the presence of DOPA on the AFM tip by measuring pull-off force on a pristine TiO_2 surface at neutral $p\text{H}$. The DOPA- TiO_2 force-distance (F - D) curves are shown in Fig. 9(a) (black F - D curves, 748 and 812 pN, respectively) and confirm the presence of a single DOPA residue on the AFM cantilever. The substrate was subsequently replaced with a mucin coated TiO_2 substrate and additional F - D curves obtained using the same tip at $p\text{H}$ values of 4.5, 6.0, 7.4, and 8.5. Due to the single molecule presence of DOPA on the AFM tip, the probability of detecting a DOPA-mucin interaction force when the tip was brought into contact with the mucin surface was observed to be less than 15%, a value that is consistent with our previous results.²⁹ Thus, most F - D curves exhibited no observable pull-off force, a common feature of single molecule experiments of this type.³³

For the tip-surface contacts where a clear DOPA-mucin interaction was observed during retraction [Fig. 9(a), red F - D curves], the F - D curves were characterized by a gradual

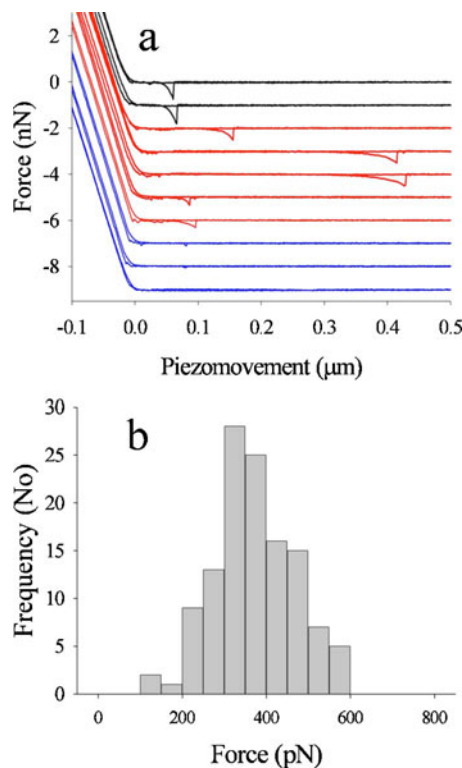


FIG. 9. Single molecule AFM results for interaction of DOPA with mucin. (a) Representative force-distance curves of DOPA-mucin interaction at $p\text{H}$ of 7.4. The AFM cantilever was first confirmed to contain PEG tethered N -Boc-DOPA by obtaining F - D curves on TiO_2 (black), revealing the expected ~ 800 pN pull-off force (Ref. 29). After changing the substrate to mucin coated TiO_2 , DOPA-mucin interactions were revealed by force signals observable at pull-off distances of up to 400 nm or more (red). DOPA free control AFM cantilevers prepared with methoxy terminated PEG showed only weak interactions with mucin (blue). (b) Force histogram of DOPA-mucin interaction force. Statistical analysis revealed an average force value of 371 ± 98 pN ($n=121$, pooled data for all $p\text{H}$ values tested).

increase in force with increasing distance from the surface, culminating in a pull-off event followed by a rapid decrease to zero force. The interaction was apparently reversible, as similar F - D curves were observed upon repeated contacts between the tip and the mucin surface. This reversible property facilitated collection of a large number of F - D curves, from which a force histogram was prepared as shown in Fig. 9(b). The mean DOPA-mucin pull-off force at $p\text{H}$ of 7.4 was determined to be 356 ± 108 pN ($n=60/400$). Consistent with the OWLS results for mucoadsorption of $\text{PEG}-(\text{DOPA})_4$ (Fig. 7), the pull-off force was found to be independent of $p\text{H}$ as summarized in Table I and the average over all $p\text{H}$ values was found to be 371 ± 98 pN ($n=121/1058$). The pull-off events were clearly attributed to the presence of DOPA, as control AFM tips prepared with only methoxy terminated PEG (2 kDa) exhibited very weak interactions (59 ± 18 pN) with a fairly low adhesion probability (4.6%) [Fig. 9(a), blue F - D curves, and Table I].

An interesting feature of the F - D curves is the large distance at which the DOPA-mucin pull-off event was observed [Fig. 9(a), red F - D curves, and Fig. 10], which ranged from 59 to 428 nm from “hard” tip-surface contact. This observa-

TABLE I. Mean pull-off force for DOPA-mucin interaction as a function of pH.

pH	Force (pN)	N_{obs}^a	N_{total}^b
4.5	366±94	25	250
6.0	392±83	27	340
7.4	356±108	60	400
8.5	418±76	9	68
Pooled ^c	371±98	121	1058
Control ^d	59±18	13	280

^a N_{obs} =number of *F-D* curves exhibiting pull-off event.

^b N_{total} =total number of *F-D* curves performed.

^cPooled=pooled results for all pH values.

^dControl=no DOPA, pooled results for all pH values.

tion is indicative of a very high mass molecule tethered between the AFM tip and the TiO₂ surface. Given that the average end-to-end distance of a fully extended PEG chain of mass of 3.4 kDa is less than 40 nm, and the magnitude of the pull-off force was inconsistent with that observed for DOPA-TiO₂,²⁹ we eliminated the possibility that the pull-off event represented DOPA interacting with the underlying TiO₂ surface. We therefore interpret the extraordinarily large observed pull-off distances as arising from extension of the mucin protein, mediated through the interaction between DOPA and mucin.

The branched PEG polymer used in this study may have an architecture conducive to mucoadhesion through interpenetration of the PEG-(DOPA)₄ arms with mucin chains;¹ however, our results cannot be explained by architecture alone because PEG-(NH₂)₄ possessed the same architecture but exhibited low mucoadsorption. Thus it is likely that the mucoadsorptive behavior originates from chemical interactions between DOPA and mucin. DOPA is a catecholic amino acid that is capable of a great variety of noncovalent and covalent interactions with organic species.^{29,34,35} Although the structure and composition of mucin proteins are not yet fully understood, mucins have heavily O-glycosylated tandemly repeated core protein domains, and associate into very high mass multimers through interchain disulfide bonds.³⁶ BSM

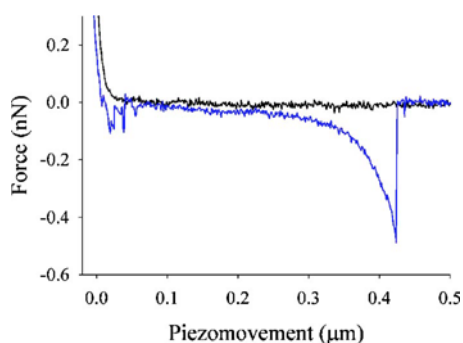


FIG. 10. Detailed example of *F-D* curve showing approach (black) and retraction (blue) for interaction of DOPA with mucin at pH of 7.4. The retraction curve deviated from the approach curve beginning at short distances and culminated in separation of DOPA from mucin at an extension of greater than 400 nm, after which the force returned to zero.

has been reported to have molar masses above 1×10^6 Da,³⁷ which may explain the long pull-off distances observed for DOPA-mucin interactions.

As to the chemical basis of the DOPA-mucin interaction, we can immediately rule out covalent bond formation, as the magnitude of the pull-off force is several times lower than necessary to break a covalent bond,³⁸ and the reversibility observed in the DOPA-mucin interaction also argues against covalent bond formation. On the other hand, it is noted that the measured interaction force between DOPA and mucin is quite large and over two times greater than that measured for interaction between a mucin peptide fragment and its antibody.^{39,40} At this time we can only speculate that hydrogen bonding, hydrophobic interactions, pi electron interactions, and physical chain entanglements could independently or cooperatively contribute to the interaction between DOPA and mucin. Further work will be necessary to fully elaborate the details, and it is likely that DOPA interacts differently with the protein backbone and the glycosylated side chains.

IV. SUMMARY

We have demonstrated significant enhancement of mucoadsorption of PEG by simple end group functionalization with DOPA. Single molecule AFM measurements of the interaction force between DOPA and mucin revealed a surprisingly strong interaction between DOPA and mucin, although determining the origin of this interaction will require further study. Nevertheless, the DOPA modified PEG polymer performed as well or better in mucoadhesion compared to existing polymers known for their mucoadhesive properties, and the mucoadhesion of DOPA was found to be pH independent. The dramatic increase in mucoadsorption of PEG upon functionalization of end groups with DOPA is remarkable when considering that the DOPA content of PEG-(DOPA)₄ is quite low (~6 wt %), demonstrating the influence of DOPA on mucoadsorption. Although the mucoadhesive behavior of PEG-(DOPA)₄ will require confirmation through future *in vitro* and *in vivo* experiments with mucosal tissue, these and other DOPA modified polymers appear to be suitable for use in drug delivery to mucosal tissue.

ACKNOWLEDGMENTS

The authors thank Bruce P. Lee for providing the PEG-(DOPA)₄ used in this study and Jeffrey L. Dalsin for the TiO₂ waveguide substrate coatings. Support for this research was provided by the National Institutes of Health under Grant No. DE 14193.

¹N. A. Peppas and Y. Huang, *Adv. Drug Delivery Rev.* **56**, 1675 (2004).

²A. Bernkop-Schnurch, *Adv. Drug Delivery Rev.* **57**, 1553 (2005).

³A. Ludwig, *Adv. Drug Delivery Rev.* **57**, 1595 (2005).

⁴M. I. Ugwoke, R. U. Agu, N. Verbeke, and R. Kinget, *Adv. Drug Delivery Rev.* **57**, 1640 (2005).

⁵N. Salamat-Miller, M. Chittchang, and T. P. Johnston, *Adv. Drug Delivery Rev.* **57**, 1666 (2005).

⁶C. Valenta, *Adv. Drug Delivery Rev.* **57**, 1692 (2005).

⁷V. Grabovac, D. Guggi, and A. Bernkop-Schnurch, *Adv. Drug Delivery Rev.* **57**, 1713 (2005).

⁸J. Cleary, L. Bromberg, and E. Magner, *Langmuir* **20**, 9755 (2004).

- ⁹V. R. Sinha, A. K. Singla, S. Wadhawan, R. Kaushik, R. Kumria, K. Bansal, and S. Dhawan, *Int. J. Pharm.* **274**, 1 (2004).
- ¹⁰S. Kockisch, G. D. Rees, S. A. Young, J. Tsibouklis, and J. D. Smart, *Int. J. Pharm.* **276**, 51 (2004).
- ¹¹X. Zhu, J. DeGraaf, F. M. Winnik, and D. Leckband, *Langmuir* **20**, 10648 (2004).
- ¹²K. Kafedjiiski, M. Werle, F. Foger, and A. Bernkop-Schnurch, *J. Drug Delivery Sci. and Tech.* **15**, 411 (2005).
- ¹³K. Maculotti, I. Genta, P. Perugini, M. Imam, A. Bernkop-Schnurch, and F. Pavanetto, *J. Microencapsul.* **22**, 459 (2005).
- ¹⁴J. D. Smart, I. W. Kellaway, and H. E. C. Worthington, *J. Pharm. Pharmacol.* **36**, 295 (1984).
- ¹⁵A. De Ascentiis, J. L. deGrazia, C. N. Bowman, P. Colombo, and N. A. Peppas, *J. Controlled Release* **33**, 197 (1995).
- ¹⁶N. A. Peppas and A. G. Mikos, *STP Pharma Sciences* **5**, 187 (1989).
- ¹⁷H. Takeuchi, J. Thongborisute, Y. Matsui, H. Sugihara, H. Yamamoto, and Y. Kawashima, *Adv. Drug Delivery Rev.* **57**, 1583 (2005).
- ¹⁸Y. Huang, W. Leobandung, A. Foss, and N. A. Peppas, *J. Controlled Release* **65**, 63 (2000).
- ¹⁹M. P. Deacon, S. S. Davis, J. H. Waite, and S. E. Harding, *Biochemistry* **37**, 14108 (1998).
- ²⁰J. Schnurrer and C. M. Lehr, *Int. J. Pharm.* **141**, 251 (1996).
- ²¹B. P. Lee, J. L. Dalsin, and P. B. Messersmith, *Biomacromolecules* **3**, 1038 (2002).
- ²²K. Huang, B. P. Lee, D. R. Ingram, and P. B. Messersmith, *Biomacromolecules* **3**, 397 (2002).
- ²³J. H. Waite, *Int. J. Adhes. Adhes.* **7**, 9 (1987).
- ²⁴J. H. Waite, *Ann. N.Y. Acad. Sci.* **875**, 301 (1999).
- ²⁵A. A. Ooka and R. L. Garrell, *Biopolymers* **57**, 92 (2000).
- ²⁶J. N. Hilfiker and R. A. Synowicki, *Solid State Technol.* **41**, 101 (1998).
- ²⁷J. Voros, J. J. Ramsden, G. Csucs, I. Szendro, S. M. D. Paul, M. Textor, and N. D. Spencer, *Biomaterials* **23**, 3699 (2002).
- ²⁸J. A. d. Feijter, J. Benjamins, and F. A. Veer, *Biopolymers* **17**, 1759 (1978).
- ²⁹H. Lee, N. F. Scherer, and P. B. Messersmith, *Proc. Natl. Acad. Sci. U.S.A.* **103**, 12999 (2006).
- ³⁰J. L. Hutter and J. Bechhoefer, *Rev. Sci. Instrum.* **64**, 1868 (1993).
- ³¹L. Shi and K. D. Caldwell, *J. Colloid Interface Sci.* **224**, 372 (2000).
- ³²J. Juna, J.-H. Shina, and M. Dhayal, *Appl. Surf. Sci.* **252**, 3871 (2005).
- ³³U. Dammer, O. Popescu, P. Wagner, D. Anselmetti, H.-J. Guntherodt, and G. N. Misevic, *Science* **267**, 1173 (1995).
- ³⁴B. Lee, J. L. Dalsin, and P. B. Messersmith, in *Biological Adhesives*, A. M. Smith and J. A. Callow (Springer-Verlag, Berlin, 2006), pp 257–278.
- ³⁵J. H. Waite, N. H. Andersen, S. Jewhurst, and C. Sun, *J. Adhes.* **81**, 1 (2005).
- ³⁶J. Perez-Vilar and R. L. Hill, *J. Biol. Chem.* **274**, 31751 (1999).
- ³⁷W. Jiang, D. Gupta, D. Gallagher, S. Davis, and V. P. Bhavanandan, *Eur. J. Biochem.* **267**, 2208 (2000).
- ³⁸M. Grandbois, M. Beyer, M. Rief, H. Clausen-Schaumann, and H. E. Gaub, *Science* **283**, 1727 (1999).
- ³⁹T. Sulchek, R. W. Friddle, and A. Noy, *Biophys. J.* **90**, 4686 (2006).
- ⁴⁰T. A. Sulchek *et al.*, *Proc. Natl. Acad. Sci. U.S.A.* **102**, 16638 (2005).